JCSE The Journal of Corrosion Science and Engineering
ISSN 1466-8858 Volume 15, Preprint 36 submitted 20 December 2012

The investigation on the corrosion inhibition of the mild steel by the three new hepta dentate thio Schiff bases in hydrochloric acid solution

M. Behpour*, S.M. Ghoreishi, E. Rajaei, N. Mohammadi, M. Hamadanian, M. Salavati-Niasari

Department Analytical Chemistry, Faculty of Chemistry, University of Kashan, Kashan, I. R. Iran

* Corresponding author: Mohsen Behpour

Mailing address: Ravand Street, Kashan, P.O.BOX: 87317-51167, Iran

(University of Kashan, Faculty of Chemistry, Department of Analytical Chemistry)

Fax number: +983615552935, Tel number: 00983615912375

E-mail: m.behpour@kashanu.ac.ir (M. Behpour)

Abstract

The inhibition performance of three new Schiff bases as corrosion inhibitors for mild steel in 2 M HCl have been investigated by weight loss, potentiodynamic polarization, electrochemical impedance, quantum and atomic force microscopy (AFM) methods. Potentiodynamic polarization study shows that the inhibitors are mixed type. All measurements indicate that inhibition efficiency increase with increasing at the inhibitors concentration. The adsorption of inhibitors on mild steel surface follow Langmuir adsorption isotherm. Kinetic parameters such as E_a, ΔH^*, ΔS^* have evaluated from the effect of temperature on corrosion and inhibition processes. Quantum chemical calculations are further applied to reveal the adsorption structure and explain the experimental results. Moreover, samples of mild steel are examined by AFM method.

Keywords: Mild steel; hepta dentate thio Schiff base; Corrosion; Impedance; Polarization

1. Introduction

ISSN 1466-8858 Volume 15, Preprint 36 submitted 20 December 2012

Corrosion represents a terrible waste of both resources and money. The wide spread use of mild steel is for its low cost and good mechanical property and availability. The study of mild steel corrosion phenomena has become important particularly in acidic media because of increasing of industrial applications of acid [1–4]. Among the commercially available acids, the most frequently used one is hydrochloric acid. It is used for removal of undesirable scale and rust in the metal working, cleaning of boilers and heat exchangers, etc [5-11]. Among the various methods available, the use of inhibitor is one of the most methods for protection against corrosion especially in acidic media [12–17]. Inhibitors are compounds that control, reduce or prevent reactions between a metal and its surroundings when added to the medium in small quantities. Most of well known acid corrosion inhibitors are organic compounds containing nitrogen, sulfur or oxygen atoms [18–22]. Schiff bases are the condensation product of an amine and a ketone or aldehyde with great utility in important fields such as medicine, agriculture and cosmetic products [23, 24]. Aims of this study are investigating the inhibitive action of three newly synthesized Schiff base compounds against the corrosion of mild steel in 2 M HCl solution. It is conducted by using weight loss, polarization, electrochemical impedance spectroscopy, quantum and AFM methods. The nature of inhibitor adsorption process and the effect of temperature are also studied and discussed.

2. Experimental

The three Schiff bases N-{2-[bis(2-{[(E)-1-(5-nitro-2 thienyl)methylidene]amino}ethyl)amino]ethyl}-N-[(E)-1-(5-nitro-2-thienyl)methylidene]amine (SBA), N-{2-[bis(2-{[(E)-1-(3-methyl(-2-thienyl)methylidene]amino}ethyl)amino]ethyl}-N-[(Z)-1-(3-methyl-2-thienyl)methylidene]amine (SBB), and N-{2-[bis(2-{[(E)-1-(2-thienyl)ethylidene]amino}ethyl)amino]ethyl}-N-[(Z)-1-(2- thienyl)ethylidene]amine (SBC)

ISSN 1466-8858 Volume 15, Preprint 36 submitted 20 December 2012

(Fig. 1) are synthesized according to the following procedure; The aromatic Schiff bases are prepared as follows: Tris (2-aminoethyl) amine (0.01 mol) is mixed with 25 mL distilled ethanol in a 250 mL round bottom flask, which is stirred using a magnetic stirrer. Aromatic aldehyde (0.03 mmol) dissolved in a 25 mL of distilled ethanol is added drop by drop using a dropping funnel to the above solution. The contents are refluxed for 12 h, and then cooled to room temperature. The yellow solid product is filtered, and the product is re-crystallized from ethanol. The Schiff base products are identified by physical and spectroscopic data. The results are as follows:

Anal. calcd. for SBA: $C_{21}H_{21}N_7S_3O_6$: C, 44.75; H, 3.76; N, 17.40. 1H-NMR. (400 MHz, CDCl3, internal reference TMS): 8.26 (3H, s, CH=N), 7.82 (3H, d, thiophene), 7.03 (3H, d, thiophene), 3.69 (6H, t, CH_2), 2.90 (6H, t, CH_2). Main i.r. (KBr, cm^{-1}): 1630 (C=N) Yield 78%, m.p. 168–170 $^{\circ}$C. Anal. calcd. for SBB: $C_{24}H_{30}N_4S_3$: C, 61.24; H, 6.42; N, 11.90. 1H-NMR. (400 MHz, $CDCl_3$, internal reference TMS): 8.36 (3H, s, CH=N), 7.26 (3H, d, thiophene), 6.89 (3H, d, thiophene), 3.65 (9H, s, CH_3), 2.90 (6H, t, CH_2), 2.29 (6H, t, CH_2). Main i.r. (KBr, cm^{-1}): 1628 (C=N). Anal. calcd. for SBC: $C_{24}H_{30}N_4S_3$: C, 61.24; H, 6.42; N, 11.90. 1H-NMR. (400 MHz, CDCl3, internal reference TMS): 8.36 (3H, s, CH=N), 7.26 (3H, d, thiophene), 6.89 (3H, d, thiophene), 3.65 (9H, s, CH_3), 2.90 (6H, t, CH_2), 2.29 (6H, t, CH_2). Main i.r. (KBr, cm^{-1}): 1663 (C=N).

The working electrode is prepared from mild steel with a composition (wt.%) C (0.027), Si (0.0027), P (0.009), Al (0.068), Mn (0.340), S (0.003), Nb (0.003), Cu (0.007), Ni (0.030), Ti (0.003), Cr (0.008), V (0.003) and Fe (balance). For electrochemical measurements, the metal is soldered with Cu-wire for electrical connection and embedded in epoxy resin to offer only one active flat surface exposed to the corrosive environment. Prior to all measurements, the specimens are mechanically abraded with a series of emery papers up to 2500 grade. Then it is rinsed in ethanol and double distilled water before immersion in experimental solution. The

ISSN 1466-8858 Volume 15, Preprint 36 submitted 20 December 2012

weight loss are carried out in the open to air (non-de aerated solutions) and in a double walled glass cell. The weight loss of mild steel in 2 M HCl (in mg cm^{-2} h^{-1}) with and without inhibitors are determined at different immersion times at 298 K by weighting the cleaned samples before and after hanging the coupon into 50 mL of the solution. Each test is carried out three times and the mean weight loss is reported. A three-electrode cell, consisting of mild steel working electrode (WE), a platinum counter electrode (CE), and saturated calomel electrode (SCE) as a reference electrode, is used for electrochemical measurements. The polarization curves are recorded by using an AUTOLAB PGSTAT 35 model potentiostat-galvanostat. A Pentium IV computer with GPES software processed data. Potentiodynamic polarization curves were obtained with a scan rate of 0.5 mV s^{-1} in the potential range from −150 to +150 mV relative to the E_{corr}. In order to investigate the mechanism of inhibition and calculate activation energies of corrosion process, polarization curves were obtained at various temperatures (298–338 K) in the absence and presence of 0.1 mM (for SBA) and 1.0 mM (for SBB and SBC) inhibitors. The impedance measurements are carried out at the open circuit potential in the frequency range from 100 kHz to 0.1 Hz with a signal amplitude perturbation of 5 mV by using a computer controlled potentiostat (same model of AUTOLAB which is mentioned). A Pentium IV computer and FRA software are applied for analyzing impedance data. Experiments are always repeated at least three times so that good agreement is obtained. The molecular sketches of Schiff bases are drawn using the Gauss View 3.0. All the quantum calculations are performed with complete geometry optimization by means of standard Gaussian 2003 software package. The relationship between inhibition efficiency of the molecules and their electronic properties is investigated using the B3LYP/6-311G** functional basis set. Surface morphology of the polished mild steel and mild steel after its exposure to 2 M HCl in the absence and presence of optimum concentrations of inhibitors for

2 h at 298 K is investigated through a NT-MDT multimode AFM, controlled by solver scanning probe microscope controller.

3. Results and Discussion

3.1. Weight loss studies

Table 1 shows the values of percentage inhibition efficiency (η) obtained from weight loss measurements at different concentrations of Schiff bases and at different immersion times at 298 K. From the weight loss values, the η of each concentration are calculated using the following equations:

$$\eta = \frac{w_0 - w}{w_0} \times 100 \quad (1)$$

where w_0 and w are the corrosion rate in the absence and presence of inhibitor, respectively. It has been found that inhibition efficiency of all of these compounds increases with increase concentration. The maximum inhibition efficiency for the three Schiff bases has been obtained at maximum concentration. The η for used Schiff bases are found to be in the following order: SBA > SBB > SBC

3.2. Potentiodynamic polarization measurements

Fig. 2 (a-c) shows Tafel curves obtained for mild steel in 2 M HCl with and without the three Schiff base compounds. The values of associated electrochemical parameters, i.e., corrosion potential (E_{corr}), corrosion current density (I_{corr}), cathodic and anodic Tafel slopes (b_c, b_a) and percentage inhibition efficiency (η) values are calculated from polarization curves and listed in Table 2. The percentage inhibition efficiency (η) is calculated from following equation:

ISSN 1466-8858 Volume 15, Preprint 36 submitted 20 December 2012

$$\eta = \left(\frac{I_{corr}^{\circ} - I_{corr}^{inh}}{I_{corr}^{\circ}} \right) \times 100 \quad (2)$$

where I_{corr}° and I_{corr}^{inh} are uninhibited and inhibited corrosion current densities, respectively. It is clear that anodic and cathodic current decreases in the presence of all of investigated Schiff bases and this effect increases with the increase in inhibitor concentration. It shows that the addition of inhibitor molecules reduces anodic dissolution of mild steel and also retards the hydrogen evolution reaction. This effect is attributed to the adsorption of the inhibitor on the active sites of the metal surface. According the literature, if the displacement in E_{corr} (i) is bigger than 85 mV with respect to E_{corr}, the inhibitor can be seen as a cathodic or anodic type and (ii) if displacement in E_{corr} is less than 85, the inhibitor can be seen as mixed type. At this investigation the maximum displacement in E_{corr} value is less than 85, which indicates that all studied Schiff bases are mixed type inhibitors [25, 26]. The η for used Schiff bases are found to be in the following order: SBA > SBB > SBC

3.3. Electrochemical impedance spectroscopy

The corrosion behavior of mild steel in 2 M HCl in the presence and absence of three Schiff bases is investigated by electrochemical impedance spectroscopy. The Nyquist plots of mild steel in uninhibited and inhibited acidic solutions containing various concentrations of Schiff bases are shown in Fig. 3 (a-c). The impedance parameters derived from the figures are given in Table 3. Nyquist plots are analyzed using the equivalent circuit in Fig. 4, with charge transfer resistance (R_{ct}) and the constant phase element (*CPE*), both in series with the solution resistance (R_s) which represents a single charge transfer reaction. The semicircles are observed to be depressed in to the real axis of Nyquist plot as a result of the roughness of the metal surface [27-29]. This kind of phenomenon is known as the "dispersing effect" [30]. The impedance of *CPE* is given by following equation:

ISSN 1466-8858 Volume 15, Preprint 36 submitted 20 December 2012

$$Z_{CPE} = [Y_0(j\omega)^n]^{-1} \quad (3)$$

where Y_0 is the magnitude of the *CPE*, n the *CPE* exponent (phase shift), ω the angular. When the value of n is 1, the *CPE* behaves like an ideal double-layer capacitance (C_{dl}). The correction of capacity to its real values is calculated from the following equation:

$$C_{dl} = Y_0(\omega_{\max})^{n-1} \quad (4)$$

Where ω_{max} is the frequency at which the imaginary part of impedance ($-Z_{im}$) has a maximum [31]. The data obtained from fitted spectra are listed in Table 3. Data show that the R_{ct} values increase and the calculated C_{dl} values decrease. It is well known that the capacitances inversely proportional to the thickness of the double layer [32]. The decrease in C_{dl} results from a decrease in local dielectric constant and/or an increase in the thickness of the double layer, suggesting that Schiff bases inhibit the iron corrosion by adsorption at steel/acid interface [33]. A low capacitance may result if water molecules at the electrode interface are largely replaced by organic inhibitor molecules through adsorption [32]. The percentage inhibition efficiency is calculated using charge transfer resistance as follows:

$$\eta = \frac{R_{ct}^{inh} - R_{ct}^{\circ}}{R_{ct}^{inh}} \times 100 \quad (5)$$

where R_{ct}° and R_{ct}^{inh} are the charge transfer resistance values without and with inhibitor, respectively. The inhibiting efficiencies determined by impedance are in good agreement with polarization method. The η for used Schiff bases are found to be in the following order: SBA > SBB > SBC

3.4. Adsorption isotherm

Since the corrosion inhibition process is based on the adsorption of the Schiff base molecules on the metal surface it is essential to know the mode of adsorption. The results show all of the investigated compounds agreed with the Langmuir isotherm:

ISSN 1466-8858 Volume 15, Preprint 36 submitted 20 December 2012

$$\frac{C}{\theta} = \frac{1}{K_{ads}} + C \quad (6)$$

where C concentration of inhibitor, θ is the coverage degree and K_{ads} is the adsorption equilibrium constant. To calculate the surface coverage (θ), it is assumed that the inhibitor efficiency is mainly due to the blocking effect of the adsorbed species and hence $\eta = 100 \times \theta$. The Tafel results at 298 K are used to calculate the adsorption isotherm parameters. The value of K_{ads} is related to the standard free energy of adsorption (ΔG°_{ads}) by the following equation:

$$K_{ads} = \frac{1}{55.5}\exp\left(\frac{-\Delta G^{\circ}_{ads}}{RT}\right) \quad (7)$$

where R is the gas constant and T is the absolute temperature. The value of 55.5 is the molar concentration of water in solution expressed in mol l^{-1}. The values of adsorption equilibrium constant can be obtained from the regressions between C / θ and C (Fig. 5), and the results are listed in Table 4. The Schiff bases have a slope equal to 1.1, therefore, it could be concluded that each Schiff base unit occupies more than one adsorption site on the mild steel surface. A modified Langmuir adsorption isotherm [34, 35] could be applied to this phenomenon, which is given by the corrected equation. The standard free energy of adsorption for SBA, SBB and SBC are -43.73, -39.67 and -39.37 kJ mol^{-1}. The negative values of ΔG°_{ads} reveal the spontaneity of adsorption process, strong interaction and stability of the adsorbed layer with the mild steel surface. In the literature, negative values of ΔG°_{ads} -20 kJ mol^{-1} or lower negative are attributed to the electrostatic interaction between the charged molecules and the charged metal (physisorption). When ΔG°_{ads} is between -80 to -400 kJ mol^{-1}, the interaction is chemisorptions. The calculated ΔG°_{ads} value closer to -40 kJ mol^{-1}, is between the threshold values for physical adsorption and chemical adsorption indicates that adsorption of Schiff bases on mild steel surface involves two types of interaction [36-38].

JCSE The Journal of Corrosion Science and Engineering
ISSN 1466-8858 Volume 15, Preprint 36 submitted 20 December 2012

3.5. *Effect of temperature*

The temperature can modify the interaction between the mild steel electrode and the acidic medium in the absence and presence of the inhibitors. In order to study the effect of temperature on the inhibition efficiencies of the Schiff bases, polarization experiments are conducted in the range of 308-338 K, in the absence and presence of optimum concentration of inhibitors. Values of associated electrochemical parameters and η for all the Schiff bases are given in Table 5. The corrosion current density increases with increasing temperature both in uninhibited and inhibited solutions, and the values of inhibition efficiency of the three inhibitors decrease in the temperature range studied (Table 5). For calculating activation parameters for the corrosion process, Arrhenius equation is used:

$$r = \lambda \exp(-\frac{E_a}{RT}) \tag{8}$$

$$r = \left(\frac{RT}{Nh}\right)\exp\left(\frac{\Delta S^*}{R}\right)\exp\left(\frac{-\Delta H^*}{RT}\right) \tag{9}$$

where λ is the Arrhenius pre-exponential factor, T the absolute temperature, E_a the activation corrosion energy for the corrosion process, h the Planck's constant, N the Avogadro's number, ΔS^* the entropy of activation, ΔH^* the enthalpy of activation and r is the rate of metal dissolution reaction which is directly related to corrosion current density (I_{corr}). The activation corrosion energy (E_a) at optimum concentration of Schiff bases is calculated by linear regression between ln (I_{corr}) and $1/T$ (Fig. 6) and the results are shown in Table 6. About activation energy there are two possibilities: in the first case ($E_{a,inh} > E_{a,HCl}$) the inhibitor is adsorbed on the most active adsorption sites (having the lowest energy) and the corrosion process takes place predominantly on the active sites of higher energy. In the second case ($E_{a,inh} < E_{a,HCl}$) the values of K are lower than HCl, i.e. smaller number of more active sites remain uncovered which take part in the corrosion process. The activation energy

for blank, SBA, SBB and SBC are 50.5, 74.4, 84.5 and 85.3 respectively. The results show that the values of E_a determined in solutions containing inhibitors are higher than that of blank. The increase in E_a in the presence of inhibitor may be interpreted as physical adsorption that occurs in the first stage [39, 40]. Fig. 7 shows a plot of ln (I_{corr}/T) versus 1/T. Straight lines are obtained with a slope of ($\Delta H^*/R$) and an intercept of (ln (R/Nh) + $\Delta S^*/R$) from which the values of ΔH^* and ΔS^* are calculated, and listed in Table 6. The positive signs of the enthalpies ΔH^* reflect the endothermic nature of the mild steel dissolution process and that mean the dissolution of mild steel is difficult. The negative values for ΔS* in the inhibited and uninhibited systems imply that the activation complex in the rate determining step represents association rather than dissociation step, which means that a decrease in disorder takes place on going from reactant to the activated complex [41].

3.6. Quantum chemical calculations

This is a useful approach to investigate the mechanisms of reaction in the molecule and its electronic structure level and electronic parameters can be obtained by means of theoretical calculations using the computational methodologies of quantum chemistry [42]. Some of the quantum chemical parameters such as the energies of the molecular orbital, E_{HOMO} (highest occupied molecular energy) and E_{LUMO} (lowest unoccupied molecular orbital energy), ΔE = E_{LUMO} - E_{HOMO} (energy of the gap), μ (dipole moment) have been determined for possible relations with the inhibitor efficiency of the Schiff bases molecules and listed in Table 7. The optimized molecular structures are shown in Fig. 8.

The results show that through quantum chemical calculations used in this study, the values of ΔE obtained from the B3LYP/6-311G** method is a parameter with the smaller value causes higher inhibition efficiencies of the molecule [43] which are in good correlation with experimental inhibition efficiencies. The non-linear equation is used to correlate all quantum chemical parameters (E_{HOMO}, E_{LUMO}, μ) and inhibitor concentration (C_{inh}) with the

experimental inhibition efficiencies. The non-linear model proposed by Lukovits et al. for the interaction of corrosion inhibitors with metal surface in acidic solutions has been used in this part of the study. Following equation is obtained for the three compounds.

$$E_{cal}\% = \frac{(A + B \times E_{HOMO} + C \times E_{LUMO} + D \times \mu)\sqrt{C_i}}{1 + (A + B \times E_{HOMO} + C \times E_{LUMO} + D \times \mu)\sqrt{C_i}} \times 100 \quad (10)$$

where A, B, C and D are 1.766344526, -14766.07401, 78689.39016, 569.9694344, respectively. The plot of the experimental and the calculated inhibition efficiency of the three Schiff bases are presented in Fig. 9. Highly significant multiple correlation coefficient (R^2 = 0.96) between experimental and calculated efficiencies is obtained.

3.7. Surface characterization: AFM study

Atomic force microscopy (AFM) is a powerful technique to investigative the surface morphology at nano to micro-scale and has become a new choice to study the influence of inhibitors on the generation and the progress of corrosion at the metal/solution interface. The recorded 3D images of surface topography are shown in Fig. 10. These images show rough surface for the polished mild steel and mild steel after its exposure to 2 M HCl in the absence and presence of optimum concentration of inhibitors. It is clear that the surface is more uniform in the inhibited solution than the surface in the absence of the inhibitor because the inhibitor molecules are adsorbed on the active sites and protect the metal against corrosion.

3.8. Molecular structure and inhibitor properties

The mechanism of the inhibition processes of the corrosion inhibitors under consideration is mainly the adsorption one. The process of adsorption is governed by different parameters depend almost on the chemical structure of these inhibitors. Many of the organic corrosion inhibitors have at least one polar unit with atoms of nitrogen, sulfur, oxygen and in some cases phosphorous. It has been reported that the inhibition efficiency decreases in the order to

ISSN 1466-8858 Volume 15, Preprint 36 submitted 20 December 2012

O < N < S < P. The polar unit is regarded as the reaction center for the adsorption process. The inhibition efficiency values of examined Schiff bases at a same concentration of 0.10 mM follow the order: SBA > SBB > SBC at room temperature. SBA investigated in the current work have three C=N groups, three sulfur atoms, one nitrogen atom, and three NO_2 groups. In addition, SBB and SBC have three C=N groups, three sulfur atoms, one nitrogen atom, and three CH_3 groups. The presence of the sulfur in the organic structure makes the formation of dπ–dπ bond, resulting from the overlap of 3d-electrons from Fe atom to the 3d vacant orbitals of the sulfur atom, possible and thus adsorption of Schiff bases on the metal surface is enhanced. Moreover, presence of C=N groups increase adsorption of inhibitors on the surface of mild steel. Experimental results show that the inhibition efficiency for the best inhibitor (SBA) in 0.1 mM is 96.03 %, that reason of is effect of NO_2 groups. On the other hand, Fig. 8 shows at SBA, sulfur groups cannot form intermolecular bonds. But, relatively poor performance of SBB and SBC than SBA might also be attributed to the existence of intermolecular H-bonds that are form between the neighboring molecules and sulfur groups at molecule. In this state, the structure of coverage surface will be disordered and the surface doesn't have compact layer. The results show all the groups, N, S and O each other effect on the inhibition efficiency.

4. Conclusions

All the studied Schiff bases show excellent inhibition properties for the corrosion of mild steel in 2 M HCl solution. The obtained inhibition efficiency of Schiff bases from impedance, polarization curves and weight loss have the same trend. Inhibition efficiencies are related to concentration, temperature and chemical structure of Schiff bases. The inhibition efficiency increases with increasing the concentration of the inhibitors. With increasing the temperature, the inhibition efficiency of three Schiff bases decreases. Polarization curves demonstrate that

ISSN 1466-8858 Volume 15, Preprint 36 submitted 20 December 2012

the examined Schiff bases behave as mixed type inhibitor. The results of impedance spectroscopy indicate that the double layer capacitances decrease with respect to the blank solution when these inhibitors are added. Adsorption of the Schiff bases on the mild steel surface obeys the Langmuir adsorption isotherm.

Acknowledgment

The authors are grateful to University of Kashan for supporting this work by Grant NO.1591959.

ISSN 1466-8858 Volume 15, Preprint 36 submitted 20 December 2012

References

[1] L. Larabi, Y. Harek, O. Benali, S. Ghalemb*, Progress Organic Coating*, 54, pp256–262, 2005.

[2] P. Zhao, Q. Liang, Y. Li, *Applied Surface Science*, 252, pp596–1607, 2005.

[3] M. Behpour, S.M. Ghoreishi, N. Mohammadi, N. Soltani, M. Salavati-Niasari, *Corrosion Science*, **52**, pp4046-4057, 2010.

[4] A. Ostovari, S.M. Hoseinieh, M. Peikari, S.R. Shadizadeh, S.J. Hashemi, *Corrosion Science*, **51**, pp1935–1949, 2009.

[5] T.Y. Soror, H.A. El-Dahan, N.G.E. Ammer, **15**, pp559–562, 1999.

[6] H. Ashassi-Sorkhabi, M.R. Majidi, K. Seyyedi, *Applied Surface Science*, **225**, pp176–185, 2004.

[7] X. Li, S. Deng, H. Fu, T. Li, *Electrochimica Acta*, **54**, pp4089–4098, 2009.

[8] Q.B. Zhang, Y.X. Hua, *Electrochimica Acta*, **54**, pp1881–1887, 2009.

[9] E. Machnikova, K.H. Whitmire, N. Hackerman**,** *Electrochimica Acta*, **53**, pp6024–6032, 2008.

[10] W. Li, Q. He, C. Pei, B. Hou, *Electrochimica Acta*, **52**, pp6386–6394, 2007.

[11] M.A. Amin, S.S. Abd El-Rehim, E.E.F. El-Sherbini, R.S. Bayoumi, *Electrochimica Acta*, **52**, pp3588–3600, 2007.

[12] E.S. Ferreira, C. Giacomelli, F.C. Gicomelli, A. Spinelli, *Material Chemistry and Physics*, **83**, pp129–134, 2004.

[13] S.M.A. Hosseini, M. Salari, M. Ghasemi, *Materials and Corrosion,* **60**, pp963-968, 2009.

[14] H. Akrout, S. Maximovitch, L. Bousselmi, E. Triki, F. Dalard, *Materials and Corrosion*, **58**, pp202-206, 2007.

[15] M. Behpour, S.M. Ghoreishi, N. Mohammadi, M. Salavati-Niasari, *Corrosion Science*, **53**, pp3380-3387, 2011.

[16] M. Behpour, N. Mohammadi, *Chemical Engineering Communications*, DOI:10.1080/00986445.2012.709473

[17] M. Behpour, N. Mohammadi, *Corrosion*, DOI: http://dx.doi.org/10.5006/0607.

[18] M. Behpour, N. Mohammadi, *Corrosion Science*, DOI:10.1016/j.corsci.2012.08.036.

[19] M.S. Morad, A.M. Kamal El-Dean, *Corrosion Science*, **48**, pp3398–3412, 2006.

[20] M. Behpour, S. M. Ghoreishi, M. Salavati-Niasari, B. Ebrahimi, *Material Chemistry and Physics*, **107**, pp153-157, 2008.

[21] M.G. Hosseini, M. Ehteshamzadeh, T. Shahrabi, *Electrochimica Acta*, **52**, pp3680–3685, 2007.

[22] S.k.A. Ali, M.T. Saeed, S.U. Rahman, *Corrosion Science*, **45**, pp253–266, 2003.

[23] A.H. Badawi, M.A.S. Mohamed, M.Z. Mohamed, M.M. Khowdairy, Journal of *Cancer Research Therapeutics*, **3**, pp198–206, 2007.

[24] S. K. Shukla, M.A. Quraishi, *Material Chemistry and Physics*, **120**, pp42–147, 2010.

[25] H. Ashassi-Sorkhabi, M.R. Majidi, K. Seyyedi, *Applied Surface Science*, **225**, pp176-185, 2004.

[26] A.K. Satapathy, G. Gunasekaran, S.C. Sahoo, Kumar Amit, P.V. Rodrigues, *Corrosion Science*, 51, pp2848–2856, 2009.

[27] K.F. Khaled, N. Hakerman, *Electrochimica Acta*, **49**, pp485-495, 2004.

[28] K.F. Khaled, N. Hakerman, *Material Chemistry and Physics*, **82**, pp949-960, 2003.

[29] Q. Qu, Sh. Jiang, W. Bai, L. Li, *Electrochimica Acta*, **52**, pp6811-6820, 2007.

[30] A. Igual Munoz, J. García Anton, J.L. Guinon, V. Perez Herranz, *Corrosion Science*, **49**, pp3200-3225, 2007.

[31] E. Machnikova, K.H. Whitmire, N. Hackerman, *Electrochimica Acta*, **53**, pp6024-6032, 2008.

[32] P. Li, J.Y. Lin, K.L. Tan, J.Y. Lee, *Electrochimica Acta*, **42**, pp605-615, 1997.

[33] M. Lagrenee, B. Mernari, M. Bouanis, M. Traisnel, *Corrosion Science*, **44**, pp573-588, 2002.

[34] R.F.V. Villamil, P. Corio, J.C. Rubin, S.M.L, *Journal of Electroanalytical Chemistry*, **535**, pp75-83, 2002.

[35] Sh. Cheng, Sh. Chen, T. Liu, X. Chang, Y. Yin, *Material Letter*, **61**, pp3276-3280, 2007.

[36] S.A. Ali, H.A. Al-Muallem, M.T. Saeed, S.U. Rahman, *Corrosion Science*, **50**, pp664-675, 2008.

[37] M. Behpour, S.M. Ghoreishi, N. Soltani, M. Salavati-Niasari, M. Hamadanian, A. Gandomi, *Corrosion Science*, **50**, pp2172-2181, 2008.

[38] E. Kamis, F. Bellucci, R.M. Latanision, E.S.H. El-Ashry, *Corrosion*, **47**, pp677-686, 1991.

[39] G. Achary, H.P. Sachin, Y. Arthoba Naik, T.V. Venkatesha, *Material Chemistry and Physics*, **107**, pp44-50, 2008.

[40] L. Larabi, O. Benali, Y. Harek, *Material Letter*, **61**, pp3287-3291, 2007.

[41] T. Szauer, A. Brandt, *Electrochimica Acta*, **26**, pp1209-1217, 1981.

[42] F. Kandemirli, S. Sagdinc, *Corrosion Science*, **49**, pp2118-2130, 2007.

[43] D.Q. Zhang, Z.X. An, Q.Y. Pan, L.X. Gao, G.D. Zhou, *Corrosion Science*, **48**, pp1437-1448, 2006.

ISSN:1466-8858 Volume 15, Preprint 36 submitted 20 December 2012

Figure Captions:

Fig. 1. Structures of studied Schiff bases

Fig. 2. Polarization curves for mild steel in 2 M HCl in the absence and presence of different concentration of three Schiff bases

Fig. 3. Nyquist plots for mild steel in 2 M HCl solution in the absence and presence of various concentration of three Schiff bases

Fig. 4. The equivalent circuit used to fit the obtained impedance spectra for mild steel in the absence and presence of the inhibitors

Fig. 5. Langmuir isotherm for adsorption of the three Schiff bases on the mild steel surface

Fig. 6. Plotting ln (I_{corr}) vs. $1/T$ to calculate the activation energy of corrosion process in the presence of inhibitors

Fig. 7. Arrhenius plots of ln(I_{corr}/T) versuse $1/T$ in the absence and presence of optimum concentrations of Schiff bases

Fig. 8. Optimized structures of the three Schiff bases obtained from B3LYP/6-311G** method

Fig. 9. Correlation between experimental inhibition efficiency and calculated inhibition efficiency obtained from B3LYP/6-311G** method

Fig. 10. AFM study of mild steel surface (a) polished mild steel (b) mild steel in 2 M HCl (c) Inhibited mild steel sample with optimum concentrations Schiff base SBA, (d) SBB and (e) SBC

ISSN 1466-8858 Volume 15, Preprint 36 submitted 20 December 2012

Table 1: Inhibition efficiency for various concentrations of the Schiff bases for the corrosion of mild steel after various Immersion times in 2 M HCl obtained from weight loss measurements at 25 °C

inhibitor	Immersion time (h)	2	4	6	12	24
	C_{inh} (mM)	η	η	η	η	η
SBA	0.01	82.85	86.34	88.68	89.33	90.68
	0.05	84.14	87.99	89.98	90.81	94.46
	0.10	86.73	89.31	91.51	92.95	96.03
SBB	0.01	81.81	85.39	87.46	88.43	89.61
	0.05	83.84	86.34	88.54	90.31	93.09
	0.10	84.85	88.11	89.21	90.45	94.68
	0.50	86.29	90.26	92.13	93.31	95.08
	1.00	87.88	92.03	93.29	94.46	95.32
SBC	0.01	77.79	78.75	80.17	82.95	85.53
	0.05	78.59	79.57	81.34	84.04	87.45
	0.10	79.38	80.53	82.51	84.86	87.51
	0.50	80.02	81.40	83.96	86.36	89.25
	1.00	80.79	82.29	84.26	87.72	90.93

ISSN 1466-8858 Volume 15, Preprint 36 submitted 20 December 2012

Table 2: Polarization parameters and corresponding inhibition efficiency for the corrosion of the mild steel in 2 M HCl without and with addition of various concentrations of the Schiff bases at 25 °C

Inhibitor	C_{inh} (mM)	$-E_{corr}$ (mV)	I_{corr} (µA cm^{-2})	$-b_c$ (mV dec-1)	b_a	η
Blank	-	494	128.8	68	71	-
SBA	0.01	479	16.56	65	57	87.14
	0.05	478	11.77	29	36	90.86
	0.10	478	8.93	44	38	93.06
SBB	0.01	497	17.13	27	30	86.70
	0.05	500	15.12	30	34	88.26
	0.10	490	14.18	23	21	88.99
	0.50	505	12.25	23	18	90.49
	1.00	491	6.61	14	11	94.87
SBC						
	0.01	498	18.25	13	15	85.82
	0.05	507	17.88	14	16	86.15
	0.10	506	16.84	16	20	86.92
	0.50	499	13.20	12	15	89.75
	1.00	504	7.93	8	8	93.84

ISSN 1466-8858 Volume 15, Preprint 36 submitted 20 December 2012

Table 3. Impedance parameters for the corrosion of the mild steel in 2 M HCl in the absence and presence different concentrations of Schiff bases at 25 °C

Inhibitor	C_{inh} (mM)	η	R_{ct} (Ω cm^2)	C_{dl} (μFcm^{-2})	Q (μFcm^{-2})	
					n	Y_0
Blank	-	-	37.2	70.17	0.89	131.7
SBA	0.01	83.73	228.7	11.30	0.83	228.2
	0.05	91.27	426.0	10.34	0.81	195.8
	0.10	93.21	548.0	6.49	0.77	131.0
SBB	0.01	86.13	286.1	48.74	0.82	103.0
	0.05	90.45	390.0	47.97	0.80	109.0
	0.10	91.41	433.0	46.05	0.80	990.0
	0.50	92.56	500.0	43.03	0.79	958.8
	1.00	93.01	532.0	42.98	0.78	991.9
SBC	0.01	85.73	260.6	50.03	0.80	161.4
	0.05	86.60	277.5	48.64	0.81	200.2
	0.10	88.80	332.0	48.10	0.78	195.7
	0.50	89.78	364.0	47.17	0.81	164.1
	1.00	91.23	424.0	45.93	0.81	161.9

ISSN 1466-8858 Volume 15, Preprint 36 submitted 20 December 2012

Table 4: Thermodynamic parameters obtained from polarization curves for the adsorption of Schiff bases in 2 M HCl on the mild steel at 25 °C

Inhibitor	K_{ads} (M^{-1})	R^2	$-\Delta G^{\circ}_{ads}$ (kJ mol^{-1})
SBA	8.4×10^5	0.99	43.73
SBB	1.6×10^5	0.99	39.67
SBC	1.4×10^5	0.99	39.37

ISSN 1466-8858 Volume 15, Preprint 36 submitted 20 December 2012

Table 5: Polarization parameters and corresponding inhibition efficiency for the corrosion of the mild steel in 2 M HCl without and with addition of optimum concentrations of the Schiff bases at different temperatures

Inhibitor	T (K)	$-E_{corr}$ (mV)	I_{corr} (μA cm^{-2})	$-b_c$ (mV dec^{-1})	b_a	η
Blank	298	494	128.8	68	71	-
	308	493	184.7	170	202	-
	318	479	486.5	104	100	-
	328	474	674.8	142	184	-
	338	482	1361.0	31	32	-
SBA	298	478	8.9	44	38	93.06
(0.10 mM)	308	501	18.0	29	23	90.23
	318	507	49.1	35	37	89.90
	328	493	92.3	24	26	86.33
	338	468	337.8	27	30	75.20
SBB	298	491	6.6	14	11	94.87
(1.00 mM)	308	505	15.9	37	36	91.40
	318	510	44.1	185	126	90.95
	328	503	96.6	181	130	85.69
	338	519	287.9	138	237	78.86
SBC	298	504	7.9	8	8	93.84
(1.00 mM)	308	510	18.6	84	31	89.91
	318	505	53.0	42	47	89.10
	328	498	88.3	28	28	86.90
	338	475	267.3	71	73	80.37

ISSN 1466-8858 Volume 15, Preprint 36 submitted 20 December 2012

Table 6: Activation parameters of dissolution reaction of the mild steel in 2 M HCl solution containing optimum concentrations of studied Schiff bases

Inhibitor	C_{inh} (mM)	E_a (kJ mol^{-1})	ΔH^* (kJ mol^{-1})	$-\Delta S^*$ (J mol^{-1} K^{-1})
Blank	-	50.5	47.42	161.02
SBA	0.10	74.4	71.51	102.84
SBB	1.00	84.5	81.83	72.01
SBC	1.00	85.3	82.51	67.26

ISSN 1466-8858 Volume 15, Preprint 36 Submitted 20 December 2012

Table 7: Quantum chemical parameters of the Schiff bases obtained from B3LYP/6-311G** method

Parameters	Inhibitor		
	SBA	SBB	SBC
E_{HOMO} (eV)	-0.22844	-0.23029	-0.23256
E_{LUMO} (eV)	-0.13458	-0.05580	-0.05556
ΔE (eV)	0.09386	0.17449	0.17700
μ (D)	14.8681	5.8770	5.6415

ISSN 1466-8858 Volume 15, Preprint 36 submitted 20 December 2012

Fig. 1

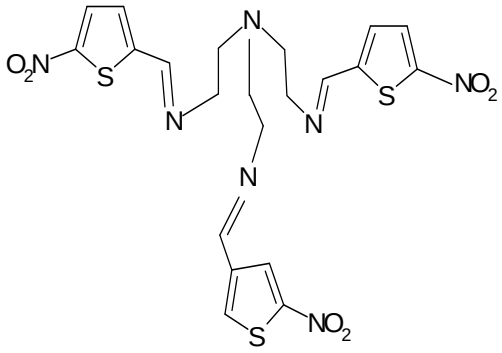

(SBA):N-{2-[bis(2-{[(E)-1-(5-nitro-2-thienyl)methylidene]amino}ethyl)amino]ethyl}-N-[(E)-1-(5-nitro-2-thienyl)methylidene]amine

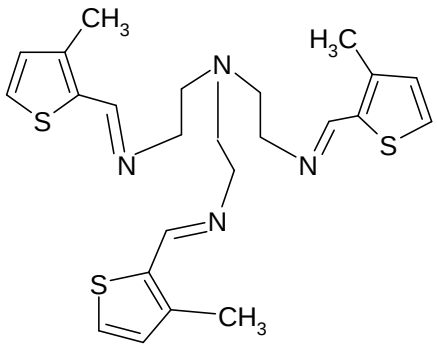

(SBB):N-{2-[bis(2-{[(E)-1-(3-methyl(-2-thienyl)methylidene]amino}ethyl)amino]ethyl}-N-[(Z)-1-(3-methyl-2-thienyl)methylidene]amine

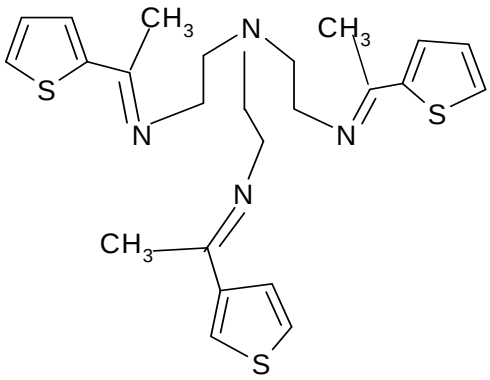

(SBC):N-{2-[bis(2-{[(E)-1-(2-thienyl)ethylidene]amino}ethyl)amino]ethyl}-N-[(Z)-1-(2-thienyl)ethylidene]amine

JCSE The Journal of Corrosion Science and Engineering
ISSN 1466-8858 Volume 15, Preprint 36 submitted 20 December 2012

Fig. 2

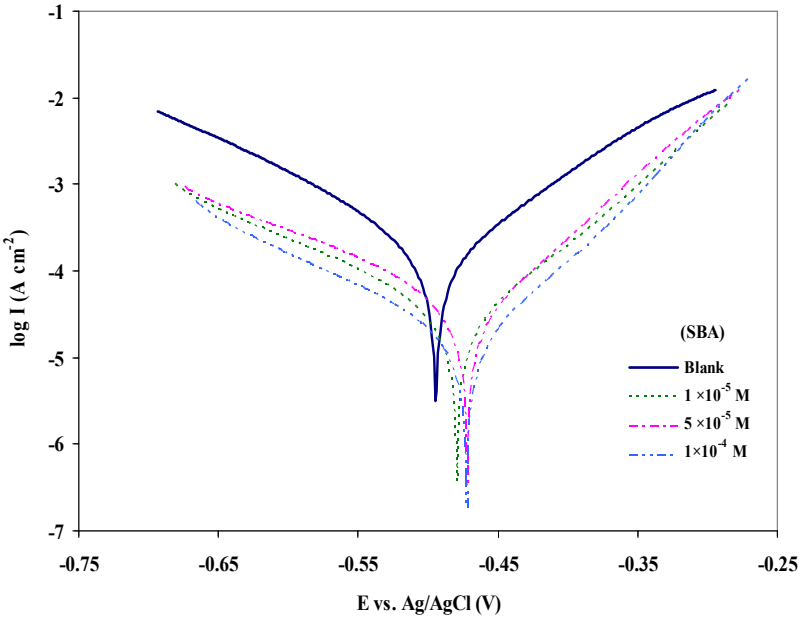

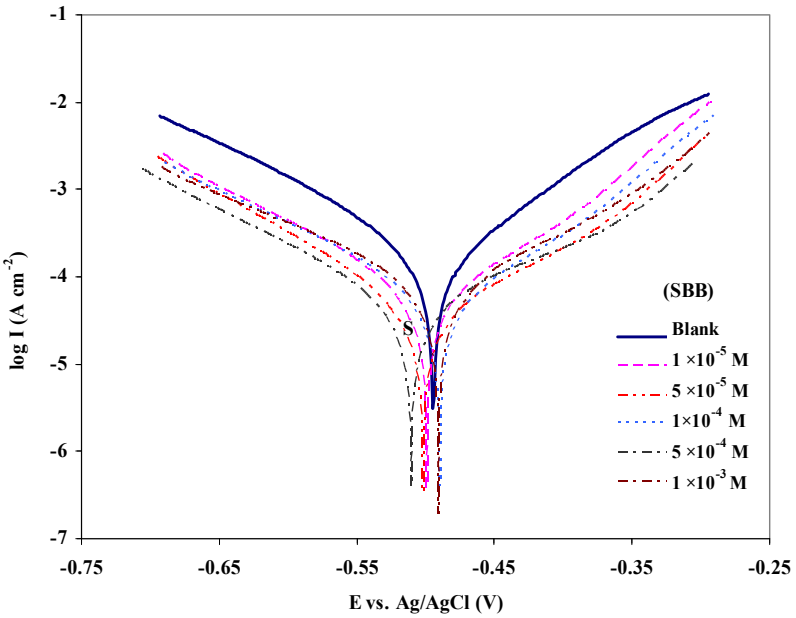

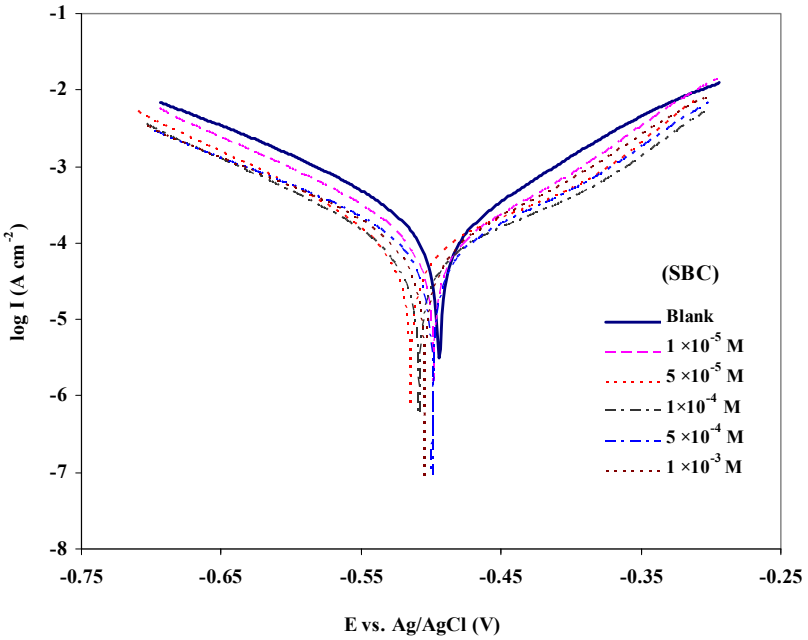

JCSE The Journal of Corrosion Science and Engineering
ISSN 1466-8858 Volume 15, Preprint 36 Submitted 20 December 2012

Fig. 3

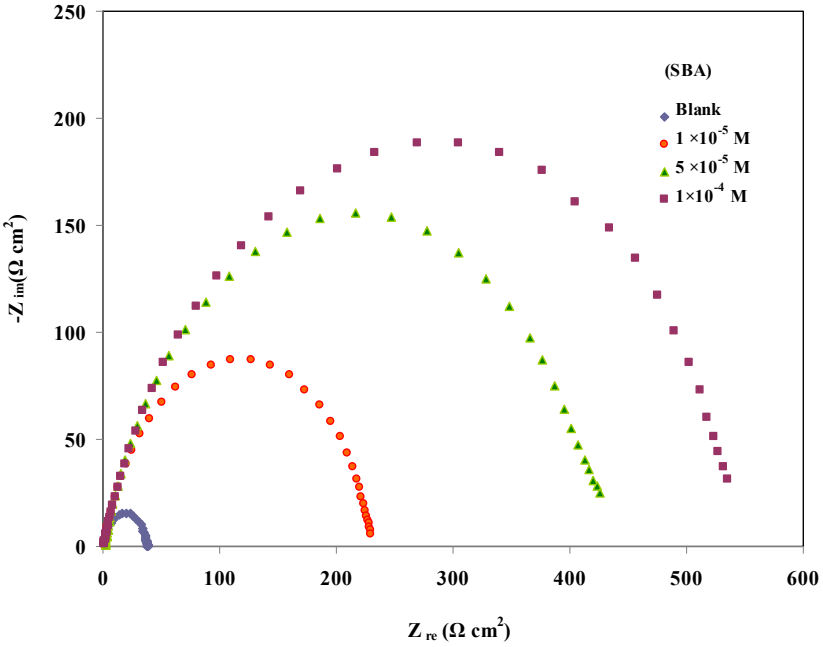

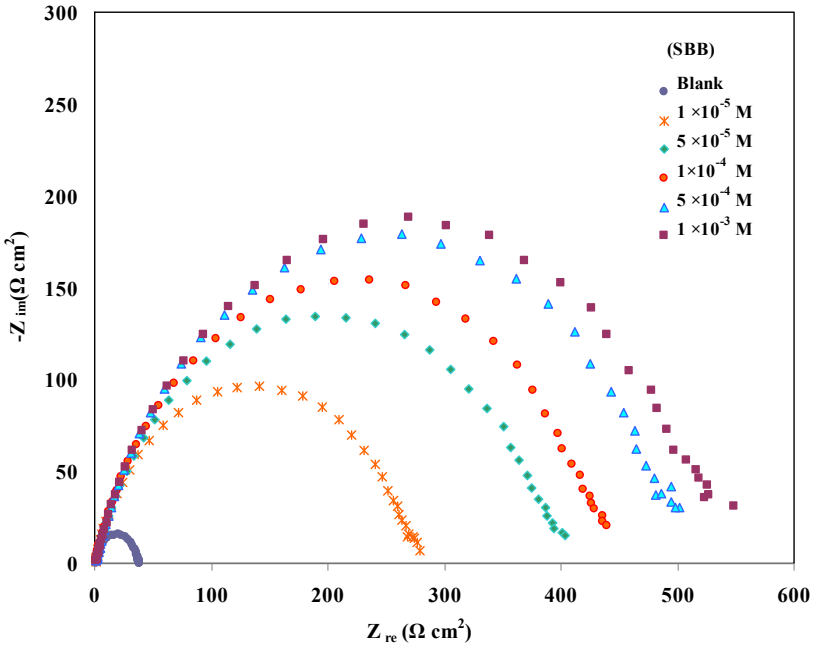

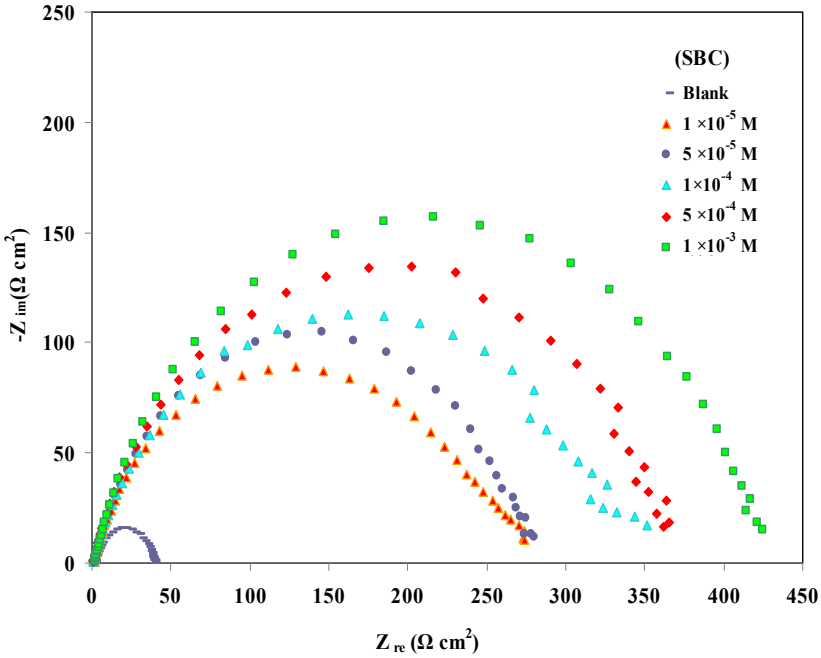

ISSN 1466-8858 Volume 15, Preprint 36 submitted 20 December 2012

Fig. 4

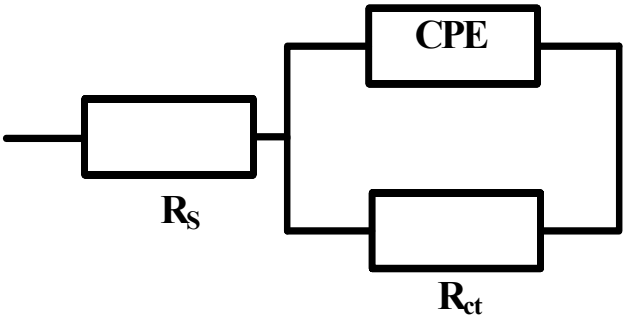

ISSN 1466-8858 Volume 15, Preprint 36 submitted 20 December 2012

Fig. 5

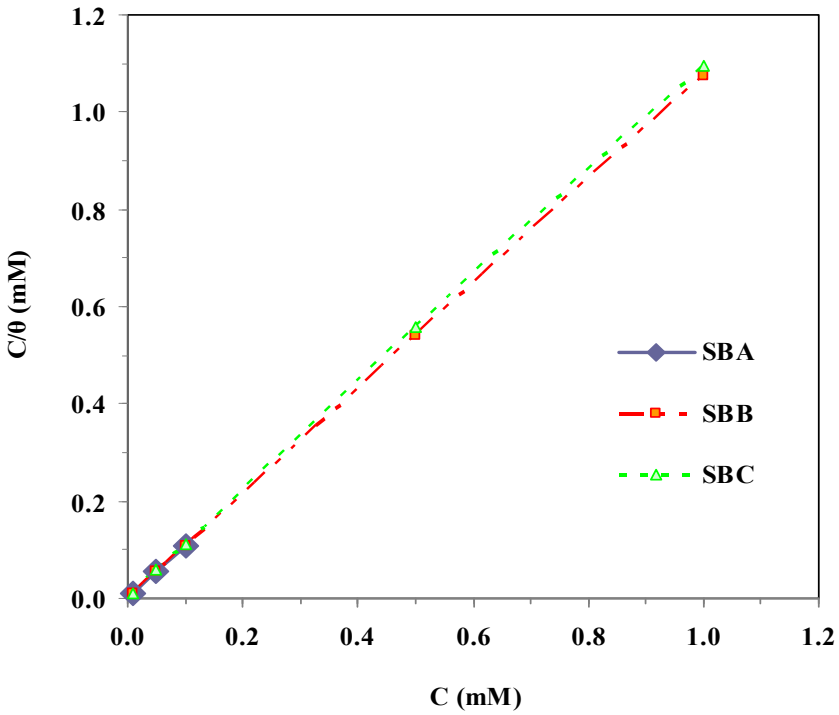

ISSN 1466-8858 Volume 15, Preprint 36 submitted 20 December 2012

Fig. 6

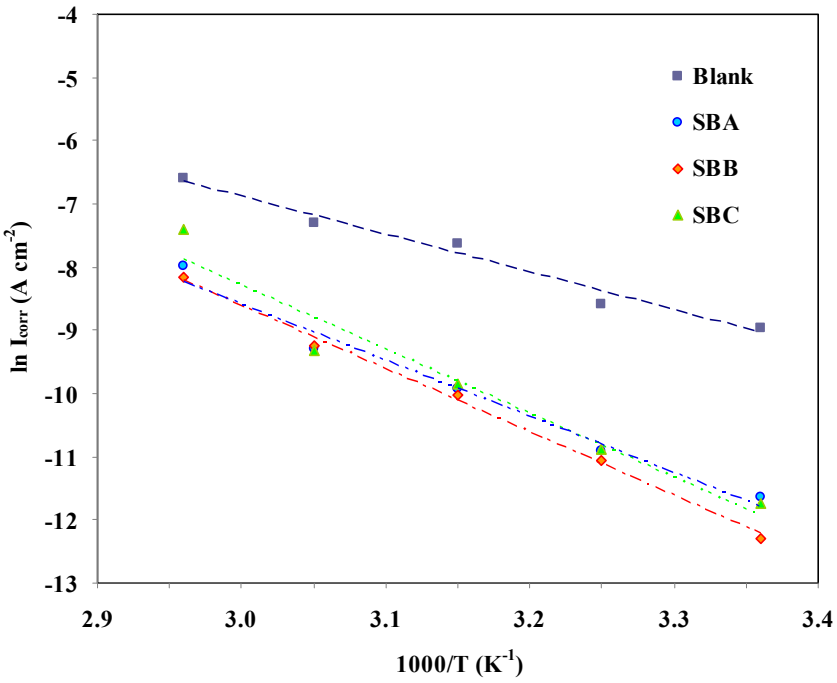

ISSN 1466-8858 Volume 15, Preprint 36 submitted 20 December 2012

Fig. 7

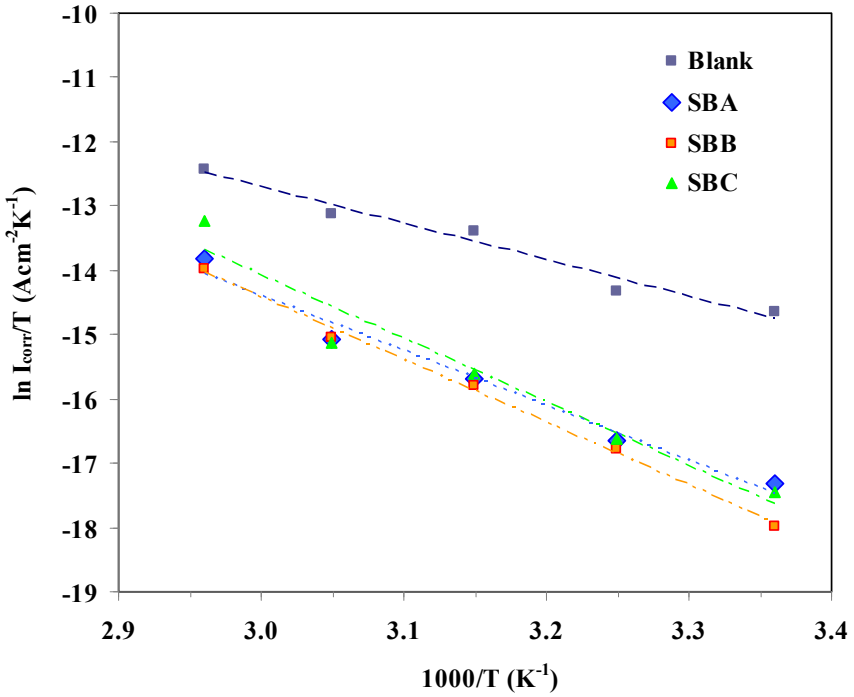

ISSN 1466-8858 Volume 15, Preprint 36 submitted 20 December 2012

Fig. 8

SBA

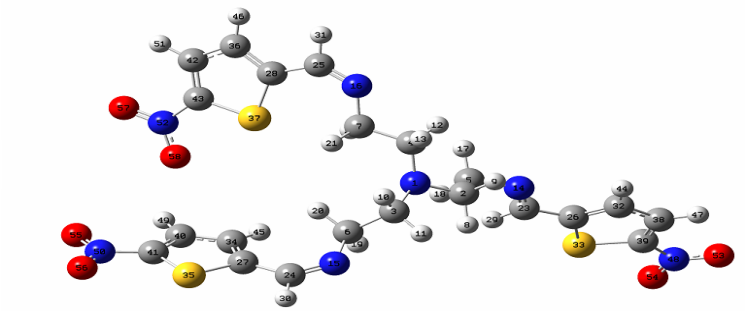

SBB

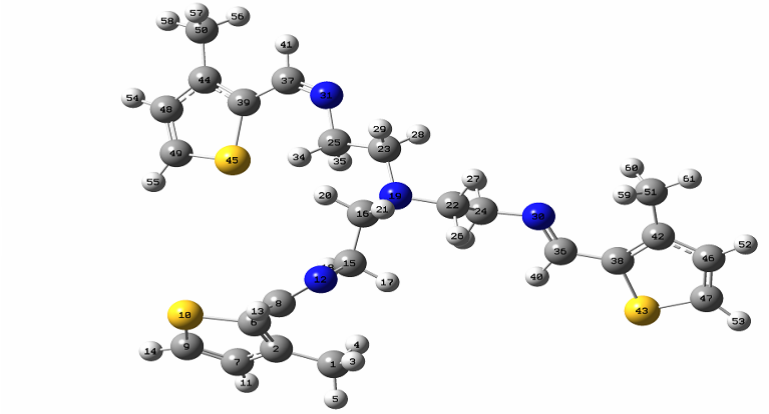

SBC

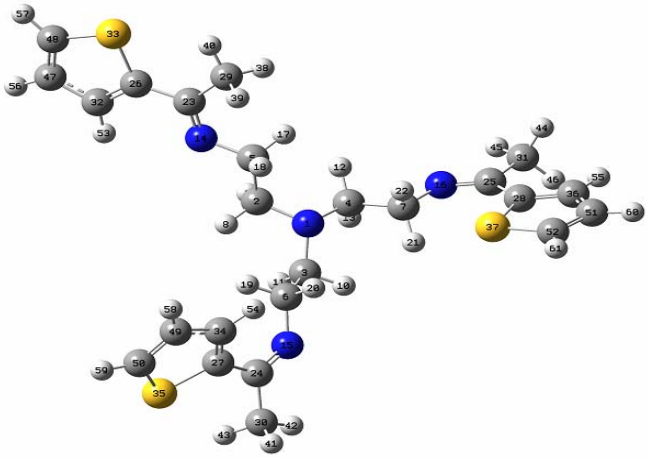

ISSN 1466-8858 Volume 15, Preprint 36 submitted 20 December 2012

Fig. 9

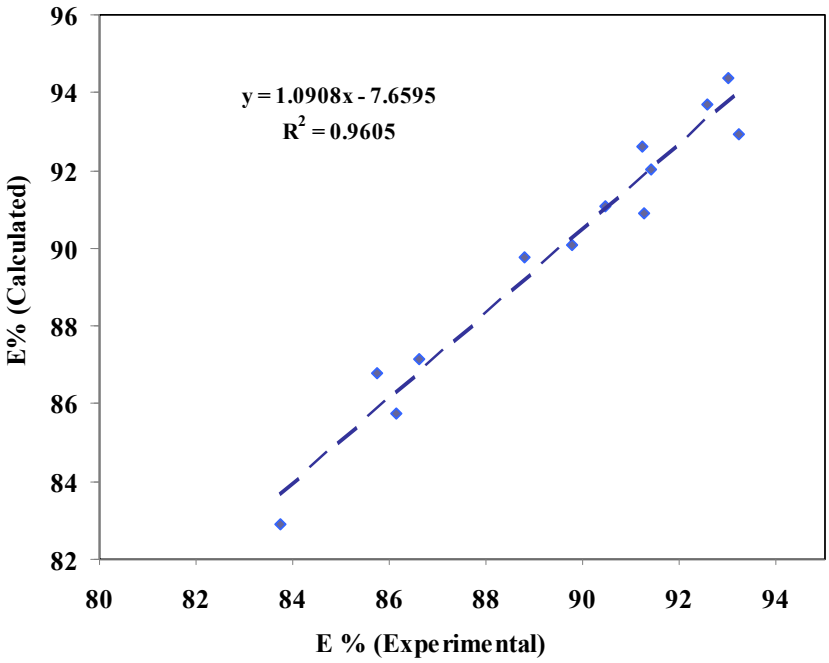

ISSN 1466-8858 Volume 15, Preprint 36 submitted 20 December 2012

Fig. 10

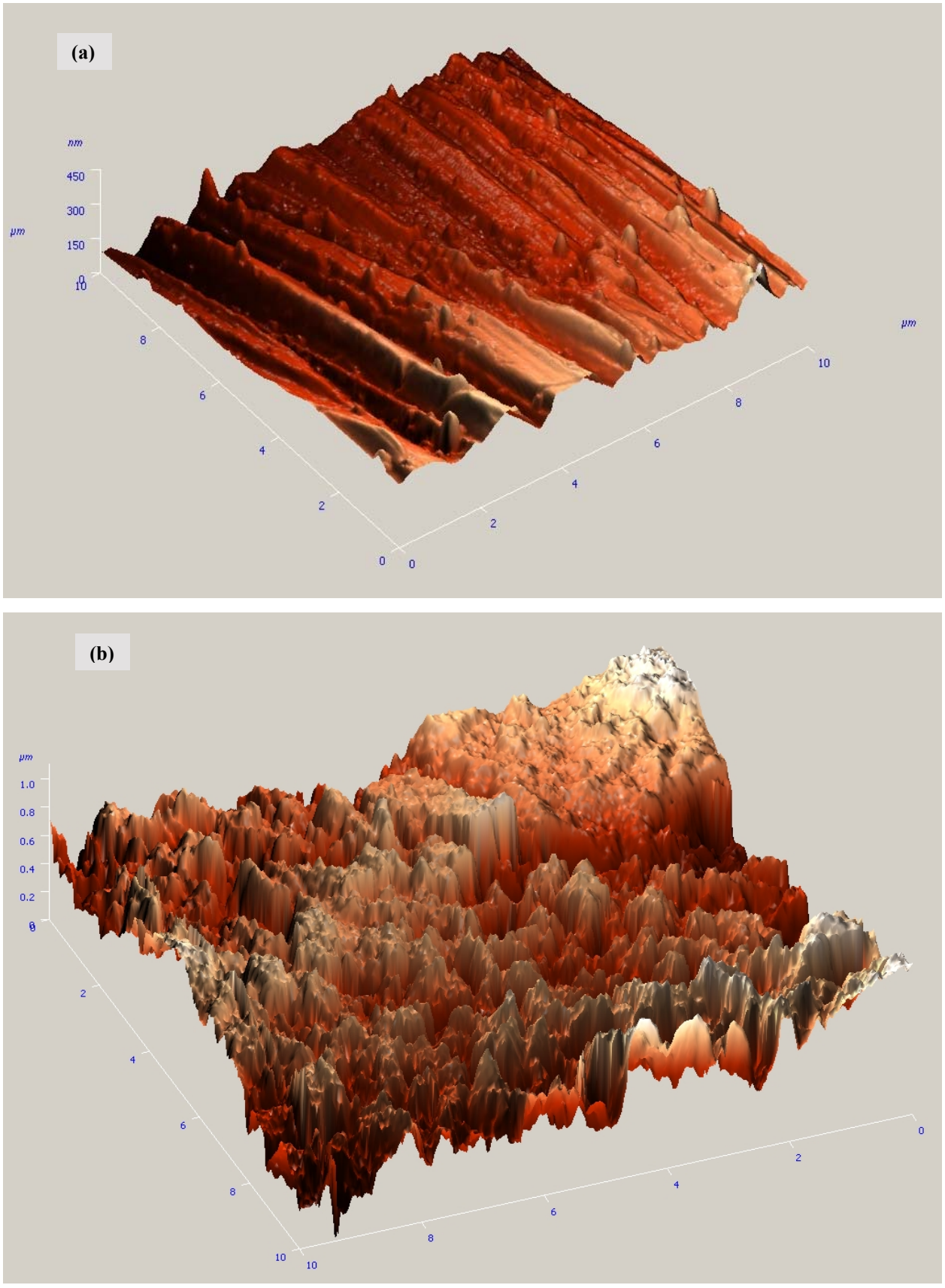

JCSE The Journal of Corrosion Science and Engineering
ISSN 1466-8858 0 December 2012